

## Supporting Information

### **Mechanochemically mediated electrosynthesis: Unveiling a New Pathway for Redox Reactions under Mechanochemical Conditions**

Mennatullah M. Mokhtar, Tom Heppler, and James Mack

Department of Chemistry, University of Cincinnati, 301 Clifton Court, Cincinnati, Ohio 45221,  
United States

## Table of Contents

1. General information.....	3
2. Mechanoelectrochemical cell designs .....	4
2.1 MEC design [4].....	4
2.2. MEC design [5].....	7
2.3 MEC design [6].....	9
2.4 MEC design [7].....	10
2.5 MEC design [8].....	15
<b>2.5.1 Test the reaction reversibility .....</b>	<b>16</b>
2.6 MEC design [9].....	19
3. Reaction procedure .....	23
3.1 General procedure for Mechanochemically mediated electroreduction for benzophenone and halogenated aromatic substrates. ....	23
3.2 General procedure for Mechanochemically mediated electrosynthesis of sulfonamides....	23
3.3 Electrode cleaning process .....	24
4. NMR characterization and spectra.....	25
5. Mass Spectrometry data.....	28
6. Green metrics calculation .....	38
6.1 Atom Economy (AE).....	38
6.2 Reaction Mass Efficiency (RME).....	38
6.3 Process Mass Intensity (PMI).....	39

6.4 Calculations for Oxidative coupling for sulfonamide synthesis procedure.....	39
7. Reference .....	39

## 1. General information

All reagents were purchased from Sigma Aldrich, TCI, and Arcos Organics. Acetonitrile (ACS,  $\geq 99.5\%$ ), utilized for mechano-electrochemical reactions, was sourced from Sigma Aldrich without additional purification, drying, or degassing. Water used in mechano-electrochemical reactions was obtained in deionized form from a tap. Milling reactions were exclusively conducted in a Spex8000M Mixer Mill. Spex 8000M Mixer/Mill (Spex SamplePrep), is designed as a single oscillation-frequency mill. However, we modified it by replacing the stock motor with a Marathon Y502 motor and interfaced this with a Frenic Mini Inverter (Fuji Electric FRNF50C1S-6U) to enable precise control of the motor's frequency. The raw materials used for the mechano-electrochemical cells, including stainless steel, graphite, and Delrin, were sourced from McMaster Carr®. Additionally, 3/16" stainless steel balls and PTFE balls were purchased from McMaster Carr®. NMR spectra ( $^1\text{H}$  and  $^{13}\text{C}$ ) were processed using a Bruker Avance 400 MHz spectrometer, and chemical shift values are reported in ppm on the  $\delta$  scale. MestReNova 9.0.1 software was employed for analyzing NMR data. Products were characterized by comparing their corresponding  $^1\text{H}$  NMR and  $^{13}\text{C}$  NMR spectra with literature. GC analyses were conducted on a GC-MS combination: Hewlett-Packard 6890 series GC-MS equipped with a Zebron ZB-5, 15 mm x 0.25 mm x 0.25 mm column. Normal Phase TLC was performed using silica gel plates obtained from Silicycle and analyzed under UV light. Flash column chromatography utilized a Combiflash® Automated Flash Column Chromatography system with RediSep Rf Gold® high-performance

flash columns (fine spherical silica gel 20-40  $\mu\text{m}$ ). Deuterated chloroform was procured from Cambridge Isotope Laboratories, Inc., Andover, MA, and utilized without additional purification.

**For mechanochemically mediated-electrochemical reactions:** the developed iterations of mechano-electrochemical cells were designed and machined at the University of Cincinnati- 1819 Hub-Makerspace unless otherwise specified. All MEC designs were equipped with two electrodes connected to a WaveDriver 20 Bipotentiostat/Galvanostat system purchased from Pine Research instrumentation. A loose key air vent incorporated in the MEC was purchased from Ace Hardware.

## 2. Mechanoelectrochemical cell designs

### 2.1 MEC design [4]

#### Reactor Design

In this design of the MEC design, we departed from the conventional use of glassware as the vessel

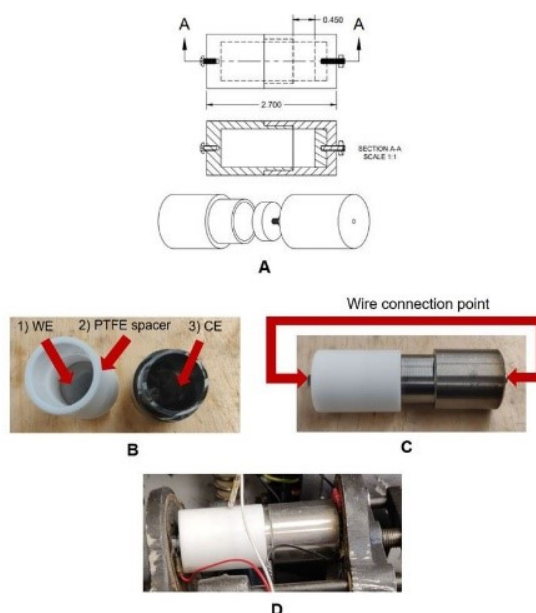


**Figure S1.** MEC 4 parts

for the electrochemical cell. Instead, we planned a configuration with two electrodes

separated by a PTFE spacer. The first electrode in this setup is a stainless- steel disc serving as the working electrode, enclosed within a PTFE cap to create separation from the second electrode—a stainless steel vessel acting as the counter electrode.(Figure S1) Our design adopts an undivided cell structure, where the volume separating the two electrodes act as the active area for the electroactive species to conduct the mechano-electrochemical reaction, the integration of a membrane to separate the counter and working electrodes would pose challenges in design implementation. The choice of stainless steel is based on its cost-effectiveness and ease of machining. We designated the smaller surface area disc as the working electrode, while the larger surface area vessel serves as the counter electrode, minimizing any potential increase in resistance for electron flow. This ensures that the half-reaction occurring at the auxiliary electrode proceeds rapidly enough to avoid limiting the process at the working electrode. The connection between the electrodes and the power supply is established using a double-ended cable with a crimp terminal (Figure S1C). Each electrode is connected to a set screw through a blind threaded hole in the electrode. The crimp terminal is affixed to the set screw and securely fastened with a nut. This ensures a robust connection, preventing any breakage during the milling process.

#### **MEC Design-4 Drawbacks**

The repeated use of the MEC design 1 led to the observation of leakage due to pressure build-up in the vial from water electrolysis, and which impose errors in quantifying reaction products. The use of stainless steel at high voltages resulted in the corrosion of the stainless-steel electrode, which was a result of using stainless steel as anode (Figure S2). The presence of a threaded hole at the bottom of the stainless-steel electrode posed challenges in securing it in the clamp assembly and keeping a consistent connection with the power source during the reaction, this resulted in the

wiring terminal being a weak point in the design. This weakness contributed to the instability of the wires and multiple disconnections.



**Figure S2.** Observed drawbacks for MEC-7.

## 2.2. MEC design [5]

### Reactor Design

In the second generation of the MEC design, two equal-sized electrodes are now separated by a PTFE spacer that includes a groove for a pseudo-reference electrode (Figure S3A). The working electrode's surface area has been increased to match that of the counter electrode. This enhancement aims to enable reactions with a higher production rate, a crucial aspect for synthetic applications. The larger surface area also facilitates increased contact between the electrodes and the electroactive species as the reaction volume decreases under milling conditions. Several issues from the first generation have been effectively addressed in this iteration. In this new design, a pseudo-reference electrode made of silver wire is introduced to aid in controlling the working electrode potential during mechano-electrochemical reactions (Figure S3C). The sampling port now serves as a venting option to eliminate leakage resulting from water electrolysis. Additionally, the stainless-steel anode has been replaced with graphite to mitigate corrosion issues. Furthermore, the new design allows for the use of graphite as the electrode material for both the anode and cathode (Figure S3D). To avoid complications in the clamp assembly and prevent connection breakage, the threaded blind hole for electrode connection to the power supply has been relocated to the side of the electrodes. This adjustment aims to ensure the success of the mechano-electrochemical reaction without any connection failures.

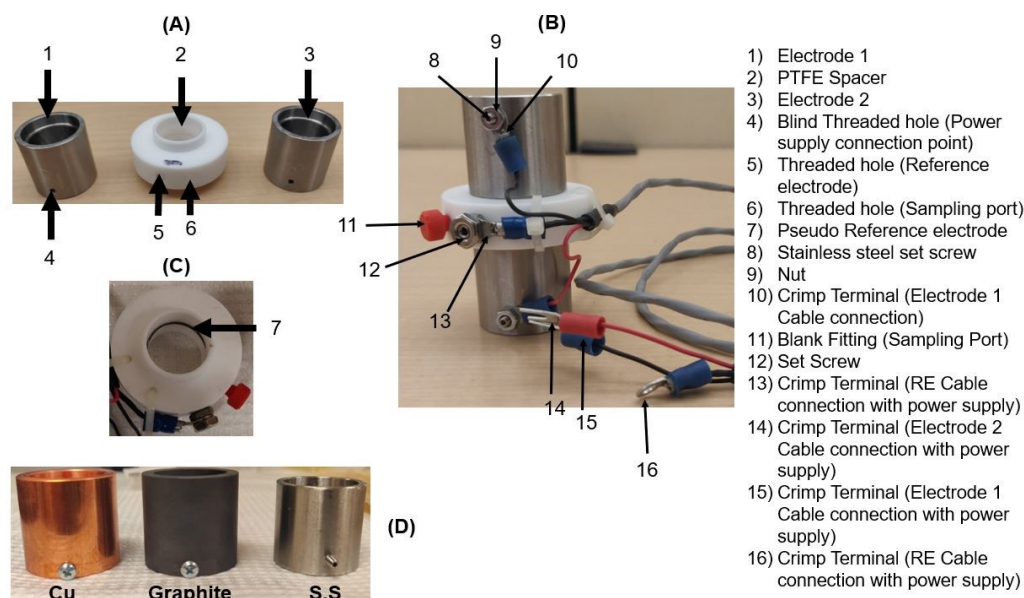


**Figure S3.** A) Parts of MEC-8 (side view), B) Assembled MEC-8, C) PTFE Spacer with vent port and a groove, D) Different electrodes materials.

### MEC Design-5 Drawbacks

The permeability of graphite has led to issues of leakage and the inability to sustain electrochemical reactions for extended periods in mechanochemistry (Figure S4).



**Figure S4.** Observed drawbacks for MEC-8.

The large surface area of the electrode poses challenges in replacing it with inert materials like platinum or gold, as these are expensive to purchase and machine on a large scale. Additionally, the substantial interelectrode gap contributes to increased resistance in the system, necessitating higher overvoltage to overcome the voltage drop.

## 2.3 MEC design [6]

### Reactor design

In the third iteration of the MEC design, two smaller equal-sized parallel electrodes are enclosed and clamped within a PTFE cap attached to a PTFE jar. The PTFE cap features two slots, appropriately sized to accommodate the width of the electrode rods, and an additional threaded slot is embedded to the side of the PTFE jar. This threaded slot allows for a stainless-steel screw to be inserted into the PTFE cap, enabling the tightening of the electrodes (Figure S5).

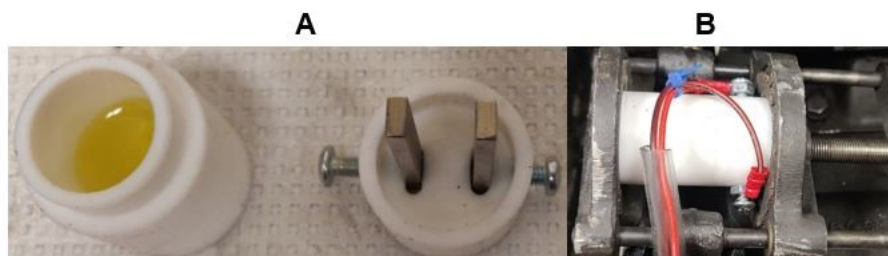


**Figure S5.** A) Parts of MEC-9 (Top view), B) Assembled MEC-9 clamped in the mill.

When setting up a reaction, ensure that the electrode is in contact with the stainless-steel screw, crimp terminal, and securely tighten the screws to hold the electrode in place. Verify that both electrodes are straight and parallel. The adoption of this design aims to address limitations observed in previous designs. The utilization of smaller-sized electrodes provides the flexibility to use inert electrodes or enclose graphite as an electrode, mitigating issues of leakage experienced in MEC design 2 when graphite electrodes were utilized under mechanical force and high voltage application resulting in extensive leakage. The parallel alignment is chosen to replicate designs reported in the literature, facilitating reproducibility, and enabling direct comparison with mechano-electrochemical outcomes.<sup>1</sup> This configuration helps minimize the inter-electrode gap, reducing resistance and voltage drop within the system.

### Reactor Design-6 Drawbacks

Efforts to test the design for benzophenone reduction were hampered by issues. The fragility of the graphite rod led to recurrent breakages whenever the cap was locked in the jar, despite multiple attempts to secure it. Modifying the solvent volume ratio inside the jar posed challenges; an increase led to leakage caused by high pressure, while a decrease resulted in suboptimal electrode contact with the solvent, leading to the absence of observed current due to elevated resistance.

#### **2.4 MEC design [7]**

In the fourth iteration of the MEC, we aimed to address challenges encountered in the previous design, striving for an improved setup conducive to exploring organic synthetic applications in mechanochemically mediated electrochemistry. We acquired a male chlorinated polyvinyl chloride (CPVC) pipe, threaded on both ends, measuring 2" long and 1/2 NPT, from McMaster Carr®. Additionally, a high-pressure brass fitting (Cap, 1/2 NPT Female) was obtained from McMaster Carr®. For the working/counter electrode, a square-shaped Platinum foil (25x25 mm, 0.025mm thick, Premion™) was procured from Thermo Fisher Scientific. The platinum foil was cut into a round shape to fit snugly inside the brass cap (Figure S6). During the reaction setup, an O-ring was employed to secure the platinum foil electrode within the brass cap, and a sealant applied to the male threads prevented content leakage during ball milling (Figure S6). In the course of the reaction, the brass cap serves as a conductive shuttle. A copper cap, equipped with a soldered wire, is connected to the power source. This configuration enables the platinum wire to act as the active electrode without a direct connection to the power source.

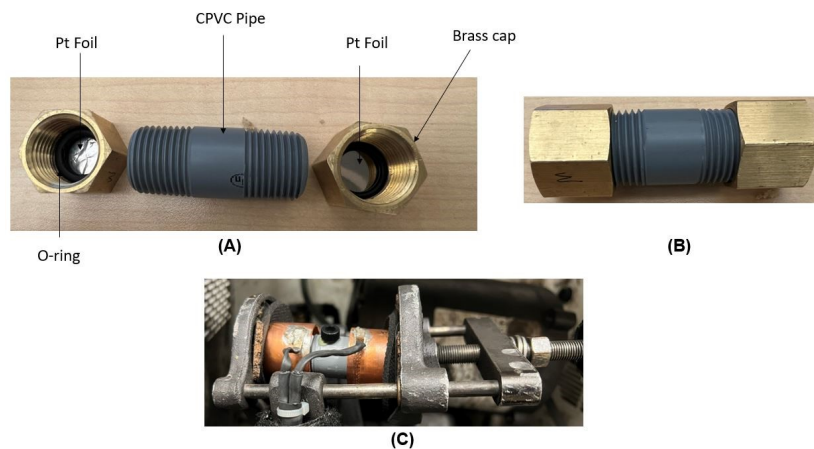


**Figure S6.** A) Parts of MEC-7(Top view), B) Assembled MEC-7, C) MEC-7 assembled in the ball mill.

### Reactor Testing

Testing the current design by filling the vial with approximately 2/3 of the total volume and milling at 17 Hz resulted in minimal conversion (Table S1, Entry 1). Conversely, conducting the reaction at 0 Hz showed better conversion, suggesting that milling at higher frequencies may not be necessary under these conditions. (Table S1, Entry 2).

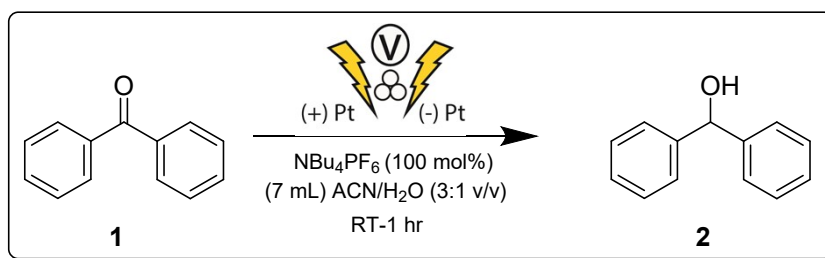


**Table S1.** Reduction conditions screening for benzophenone using MEC-7.

Entry	Voltage (V)	Milling Frequency (Hz)	Conversion to <b>2a</b> <sup>a</sup> (%)
1	-1.8	17	8
2	-1.8	0	38

<sup>a</sup>Determined by GC-MS, Reaction was performed with(1mmol) of (**1a**).

Additional trials were performed to explore the design at different frequencies and with a reduced solvent-to-volume ratio. However, these reactions did not proceed as expected. The seal formed on the threads proved insufficient to isolate the brass from the solvent, leading to the oxidation of copper and passivation on the Pt foil. This resulted in electrode fouling, reduced current efficiency in a side reaction, and the observation of leakage. This outcome prompted us to make minor adjustments to the design. The brass cap was replaced with a plastic cap, which is non-conductive even when in contact with the electrolyte solution (Figure S7). A stainless-steel screw was employed to securely hold the Pt foil inside the plastic cap, serving as the connection point to conduct electricity to the Pt electrode. This was achieved by connecting the screw to the crimp terminal of a wire linked to the power source. The recent modification resulted in a reduction of the overall internal volume compared to the previous iteration. The reduction of benzophenone using the plastic cap with Pt electrodes was performed at a lower volume at 0 Hz. In the previous reaction, the measured voltage was observed to be different from the applied voltage due to increased resistance in the system as the interelectrode gap was measured to be 5.5 cm.



**Figure S7.** A) Parts of modified MEC-7 (Top view), B) Assembled modified MEC-7.

Since the resistance is high and cannot be overcome with the current potentiostat due to maximum voltage limitations or by using more than 100 mol% of the electrolyte, we opted for a higher

potential range power source. This source lacks real-time monitoring plots of the applied current and voltage but provides a higher voltage range to drive the reaction. Upon applying 6 V with 6.5 mL of the electrolyte solution, a small amount of the corresponding alcohol (**2**) was observed. (Table S2, Entry 1) However, reducing the volume to 5.5 mL and 5 mL resulted in a decreased amount of (**2**) being observed. (Table S2, Entry 2,3)

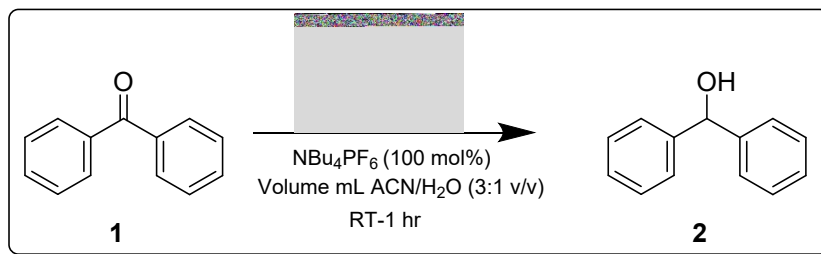


**Table S2.** Reduction conditions screening for benzophenone using modified MEC-7.

Entry	Voltage (V)	Solvent Volume (mL)	Milling Frequency (Hz)	Conversion to <b>2a</b> <sup>a</sup> (%)
1	6	6.5	0	13
2	6	5.5	0	4
3	6	5	0	3

<sup>a</sup>Determined by GC-MS, Reaction was performed with (1mmol) of (**1**).

Given our system's capability to assess the impact of milling on electrochemical reactions while minimizing solvent use, we reduced the solvent to half the internal volume of the MEC. We utilized 3.5 mL of electrolyte, applying 6 V at 0 Hz for 1 hour (Table S3 Entry 1), and observed a low current without (**2**) formation, which is expected due to the lower solvent volume. The decreased volume caused a low contact with the electrode which might be contributing to increasing the system resistance, possibly requiring milling to enhance electrode contact. Milling the reaction at 9 Hz, 17 Hz for longer durations with 6 V (Table S3, Entry 2, 3) resulted in no observed product.

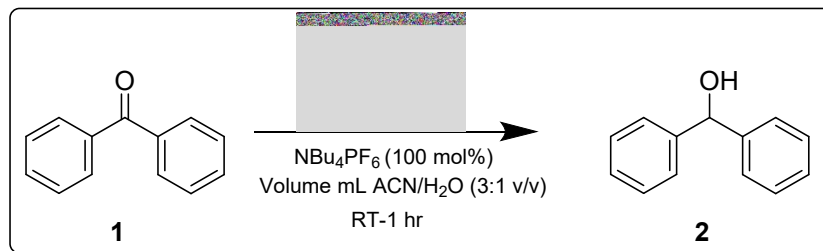


**Table S3.** Investigation of lowering solvent volume for benzophenone reduction using modified MEC-7.

Entry	Voltage (V)	Time (hr)	Milling Frequency (Hz)	Conversion to <b>2a</b> <sup>a</sup> (%)
1	6	1	0	0
2	6	1	9	0
3	6	1	17	0
4	8	7	17	0
5	16	7	17	0
6	24	7	17	0
7	30	7	17	10

<sup>a</sup>Determined by GC-MS, Reaction was performed with (1mmol) of (**1**).

Assuming increased resistance cannot be solved solely with milling but necessitates more applied voltage, consequently, we applied 8 V at 17 Hz, but it failed to form the product. (entry 4) Incrementing the voltage to 16 V, 24 V showed no trace of (**2**). (Table S3, Entry 5,6), However, applying 30 V resulted in the observation of a small amount of (**2**). (Table S3, Entry 7)

### Reactor Design-7 Drawbacks

While the initial design facilitated testing for mechanochemically mediated electrochemical reactions, several limitations became evident upon repeated reaction setups. Primarily, the use of

a platinum (Pt) foil as the electrode, while inert, posed challenges due to its limited surface area (Figure S8). This limitation hindered the electrolysis rate, necessitating extended reaction times for enhanced product yield. Additionally, the small area and thinness of the foil complicated the cleaning process, exacerbating issues related to electrode surface damage in subsequent designs.



**Figure S8.** Observed drawbacks for MEC-7, and modified MEC-7.

Upon the modification of the brass cap, the electrode foil's susceptibility to damage intensified, impacting the efficiency of electron transfer. Notably, a substantial challenge emerged in the form of a large interelectrode gap (5-6 cm), significantly exceeding the gaps reported in literature for conventional electrochemical cells. While milling showed promise in enhancing electrode contact with reduced system volume, it failed to mitigate the resistance stemming from the interelectrode gap distance. Consequently, overcoming this resistance necessitated the application of higher overpotential, or utilizing higher equivalence on electrolytes which add a layer of product isolation complexity.

## 2.5 MEC design [8]

Considering the challenges associated with bulk electrolysis experiments employing large currents, several factors significantly impact the electrode potential, especially in a two-electrode system without a reference electrode. Notably, the high current passing through the counter electrode cannot be disregarded, leading to alteration on electrode potential. The increase of the interelectrode gap, an additional concern, contributes to increased ohmic drop in the system.

Furthermore, reducing the solvent volume amplifies these challenges, affecting the submerged electrode area and potentially disrupting the connection between electrodes. These collective factors result in an elevated voltage drop, demanding more energy to drive the reaction.

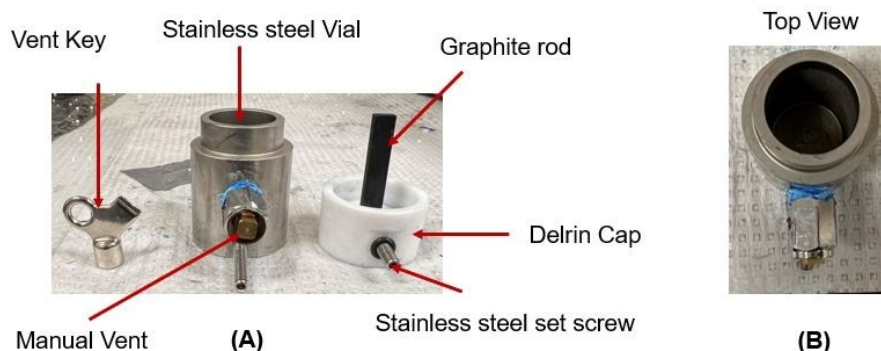


**Figure S9.** A) Parts of MEC-8 (Side view), B) MEC-8 Stainless steel electrode. (Top view)

Addressing these challenges and building upon lessons from previous designs, a novel approach was devised. The new design features a stainless-steel vial as the first electrode, incorporating a threaded hole in its body for attaching a vent to alleviate built-up pressure in the system and prevent leakages (Figure S9A). The upper section of the design utilizes a Delrin cap with a slot for the parallel placement of a graphite rod alongside the walls of the stainless-steel vial. The Delrin cap's side integrates a threaded groove accommodating a set screw, tightening the graphite rod securely in the slot (Figure S9B). This design offers the parallel alignment, decreasing the interelectrode gap, in addition to the advantage of enclosing the graphite within the stainless-steel vial, minimizing porosity-related leakage concerns, and facilitating prolonged reaction durations.

### 2.5.1 Test the reaction reversibility

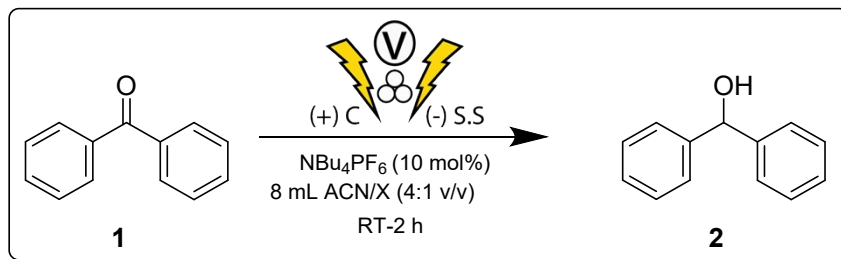


**Table S4.** Investigation of the reaction reversibility using MEC-8.

Entry	X	Milling Frequency (Hz)	Conversion to <b>1a</b> <sup>a</sup> (%)
1	EtOH	0	9
2	-	0	29
3	D <sub>2</sub> O	0	8

<sup>a</sup>Determined by GC-MS, Reaction was performed with (1mmol) of (**1a**).

These findings affirm that the proposed design is not suitable for testing with a low solvent volume under milling conditions, as minimal electrode contact is anticipated during shaking, rendering it inefficient for our study objectives. However, this design proves to be efficient for examining the system under non-milling conditions. Consequently, we will focus on studying the reversibility of the system, the design consists of a non-divided cell where the electrodes coexist in the same chamber without membrane separation. In the initial phase, benzohydroxyl (**2**) was utilized as the starting material, subjecting it to a positive voltage on the working electrode to induce oxidation. The reaction was carried out for 2 hours with application of 4.3 V, first in the presence of protonated solvent ethanol 9% conversion to **2** was observed, (Table S4, Entry 1) then to prevent the reduction of the formed product (**1**), the observed conversion of (**1**) increased to 29%. (Table S4, Entry 2) In a third trial, D<sub>2</sub>O was employed to verify that the deuterated (**1**) originated after the reduction of formed (**2**) upon oxidation of non-deuterated (**1**). The conversion was like the reaction observed in deuterated solvent which suggests that reaction is reversible. (Table S4, Entry 3) Ultimately, our objective was to devise a straightforward method for predicting the redox potential

of organic substrates within our system, accounting for the absence of a reference electrode in the MEC setup. To achieve this, we selected three substrates (4-Nitrobenzaldehyde, Nitrobenzene, Methylbenzoate) for which we measured the redox potential using the MEC-8 without the Delrin cap, and with incorporating a reference electrode in the setup while both the graphite rod and reference electrode aligned in parallel outside the mill. Cyclic voltammetry experiments were conducted to ascertain the redox potential for each substrate.

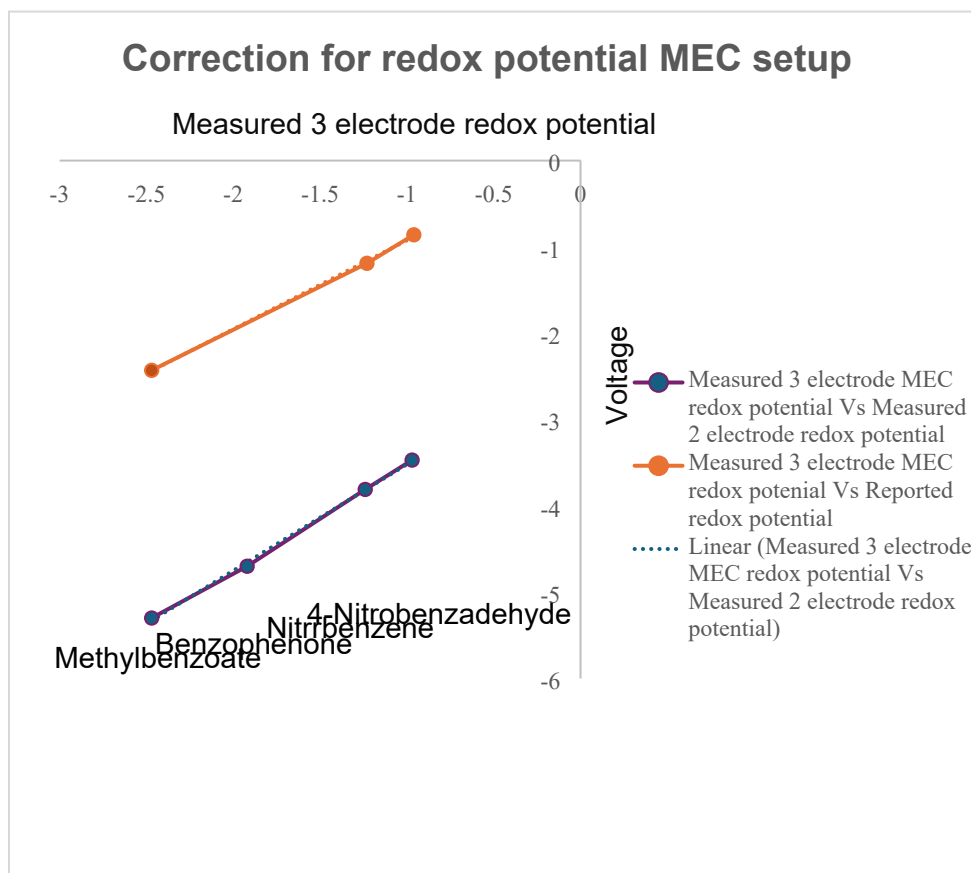


**Figure S10** Plot for redox potential correction using MEC-8.

Subsequently, we plotted these values against the reported redox potentials from the literature for comparison.<sup>2</sup> In a parallel set of experiments, using the similar 3 substrates used previously in addition to benzophenone as a fourth data point, we approximated the redox potential in the absence of a reference electrode using cyclic voltammetry (Figure S10). Despite the acknowledged

limitations of accuracy without a reference electrode, our aim was to obtain a relative estimation of the potential required for substrate reduction. This approach allowed us to establish a starting point for the redox potential, providing useful guidelines rather than relying on arbitrary values in our investigations.

## 2.6 MEC design [9]

Drawing insights from previous designs, particularly the MEC-8 design, we recognize the critical importance of electrode contact. When the goal includes minimizing solvent usage in the system and exploring the influence of mechanochemistry on reducing solvent in electrochemical reactions, it becomes imperative to align the solvent motion with the ball mill motion. This alignment ensures that the solvent maintains contact among the electrodes, preventing splashing that could lead to a complete loss of electrode contact.

In light of this understanding, we made modifications to the prior design, replacing the graphite rod with a T-shaped graphite disc. This disc is situated inside the Delrin cap, positioning its surface parallel to the stainless-steel vial. The distance between the graphite disc and the vial constitutes the active site for electrochemical reactions (Figure S11A). The presence of graphite on one side facilitates electrode contact during milling, where the eight-figure motion of the mill ensures that the liquid hits the active electrochemical site. While retaining the stainless-steel vial with a vent port, we customized the graphite disc with varying lengths corresponding to the internal volume (Figure S11C). The accompanying figure illustrates the design. Following the steps of previous trials, we have designated this modified design as our final iteration. This design is intended for fulfilling our objectives, specifically testing the minimization of solvent usage in electrochemical reactions under mechanochemical conditions. Additionally, we aim to explore the impact of milling on enhancing substrate solubility, investigate whether solvents are necessary for electrochemical reactions under mechanochemical conditions, and examine the effects of milling on various redox reactions.

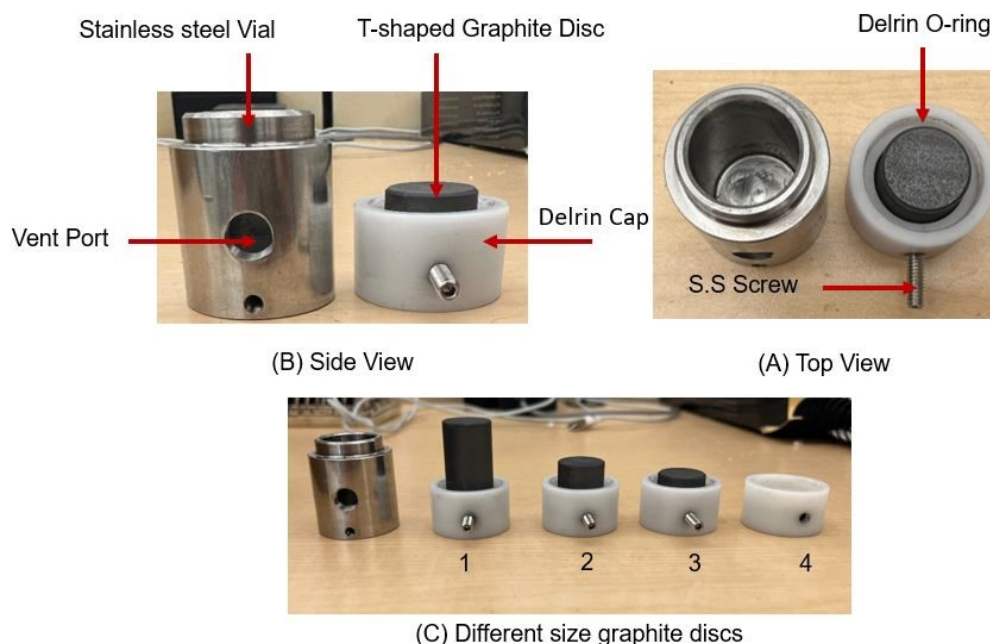


**Figure S11.** A) Parts of MEC-9 (Top view), B) Parts of MEC-9 (Side view), C) Various length of graphite electrodes.

The study initially focused on exploring the design of a mechanochemically mediated electrochemical cell for a reduction reaction. In this section, our attention shifted towards investigating the setup for an oxidation reaction. We chose to delve into the synthesis of sulfonamides due to their high value in the pharmaceutical industry. The recent report on the electrochemical synthesis of sulfonamides, achieved through the coupling of thiols and amines, served as inspiration. The simplicity and environmental friendliness of this method motivated us to assess the feasibility of mechanochemically mediated electrochemistry for the oxidative coupling of thiols and amines, aiming to produce sulfonamides under minimal solvent conditions and in a short time frame.

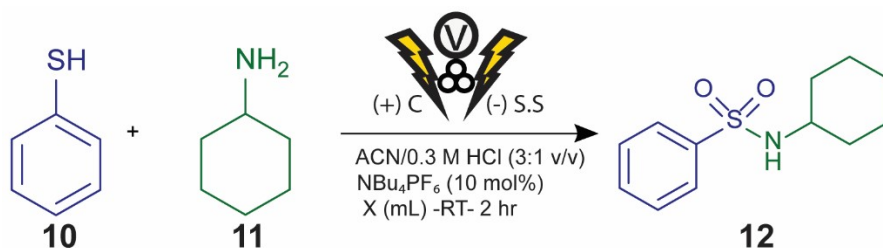


**Table S5.** Exploring lowering solvent volume for oxidative coupling of 1<sup>ty</sup> amine using MEC-9.

Entry	Applied Voltage (V)	Solvent Volume (mL)	Milling Frequency (Hz)	Conversion to <b>2g<sup>a</sup></b> (%)
1	3.2	4	0	72
2	3.2	2	0	50
3	3.2	1	0	20
4	3.2	2	17	15
5	4	1	0	19
6	4	1	17	2

We initiated the examination by evaluating the oxidative coupling of thiophenol **10** and cyclohexylamine **11**, focusing on the influence of reduced volume without milling at 0 Hz compared to milling at 17 Hz.

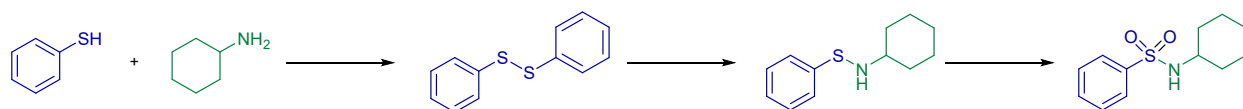


**Figure S12.** The observed intermediate of the oxidative coupling product

The reaction follows the reported mechanistic studies in the reported literature<sup>3</sup> where complete conversion of the thiol substrate to its corresponding disulfide occurs through anodic oxidation. Within five minutes, the thiophenol is consumed, and the corresponding disulfide is produced. The subsequent reaction of the aminium radical intermediate with the disulfide generates sulfenamide as observed in GC-MS then the sulfonamide product is observed. (Figure S12)

Applying voltage at 0 Hz with 4 mL of solvent yielded moderate conversions. (Table 14, Entry 1) However, halving the solvent volume to 2 mL (Table S5, Entry 2) led to a moderate reduction in conversion to 50%. When attempting to mill the reaction at 17 Hz (Table S5 Entry 4), the conversion dropped to 15%. Further reducing the solvent volume to 1 mL (Table S5, Entry 3) resulted in a dramatic reduction to 20% conversion. Exploring the impact of increased voltage with 1 mL solvent did not exhibit a notable increase in conversion (Table S5, Entry 5). Interestingly, milling the reaction at 17 Hz almost entirely abolished the conversion (S5, Entry 6). In previous findings, it is evident that high frequency is not optimal for the current system. When the MEC-9 is vigorously shaken, the liquid swiftly traverses both sides of the electrode. As the frequency increases, the electrode has limited time to maintain contact with the region featuring a small interelectrode gap. This results in a brief contact time, impacting the reaction rate. Additionally, primary amine **11** incorporated in the sulfonamide **12** led to cleavage and the formation of benzenesulfonamide.

### 3. Reaction procedure

#### 3.1 General procedure for Mechanochemically mediated electroreduction for benzophenone and halogenated aromatic substrates.

4-Bromo-benzophenone (0.9 mmol, 240 mg) or other substrates (0.9 mmol) and tetramethylammonium hexafluorophosphate ( $\text{Me}_4\text{NPF}_6$ , 0.25 mmol, 90 mg) unless otherwise noted for the electrolyte equivalence were introduced into the stainless-steel electrode vial (MEC-9). Acetonitrile was subsequently added to the MEC, followed by deionized water or ethanol at a specified concentration in a 3:1 (v/v) ratio. A stainless-steel ball (size 3/16") and a Teflon ball (size 3/16") were included. The stainless-steel electrode vial and the Delrin cap containing the graphite electrode were assembled and secured in a Spex Certiprep 8000M mixer mill. The electrodes were connected to the potentiostat set to a constant voltage/current, and the mill frequency was adjusted based on the required reaction frequency. The reaction was paused every 30 minutes to vent the MEC, addressing the evolution of hydrogen gas at the cathode and preventing pressure build-up and leakage. Once the designated reaction time concluded, the potentiostat was automatically timed to a specific duration while the mixer mill was turned off. After the reaction, the crude mixture was extracted three times with ethyl acetate (EtOAc) and dried with  $\text{MgSO}_4$ . The resulting crude mixture underwent analysis using GC-MS and  $^1\text{H-NMR}$ , with conversions calculated based on GC-MS results.

#### 3.2 General procedure for Mechanochemically mediated electrosynthesis of sulfonamides

Cyclohexylamine (1.5 mmol, 148 mg) and tetramethylammonium hexafluorophosphate ( $\text{Me}_4\text{NPF}_6$ , 0.1 mmol, 90 mg) were introduced into the stainless-steel electrode vial (MEC-9). Acetonitrile was subsequently added to the MEC, followed by HCl at a specified concentration in a 3:1 (v/v) ratio. Thiophenol (1 mmol, 110 mg) was then added to the stainless-steel electrode vial

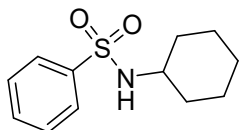
(MEC-9). A stainless-steel ball (size 3/16") and a Teflon ball (size 3/16") were included. The stainless-steel electrode vial and the Delrin cap containing the graphite electrode were assembled and secured in a Spex Certiprep 8000M mixer mill. The electrodes were connected to the potentiostat set to a constant voltage/current, and the mill frequency was adjusted based on the required reaction frequency.

The reaction was paused every 30 minutes to vent the MEC, addressing the evolution of hydrogen gas at the cathode and preventing pressure build-up and leakage. Once the designated reaction time concluded, the potentiostat was automatically timed to a specific duration while the mixer mill was turned off. After the reaction, water was introduced to the MEC-9 electrodes. The crude mixture was extracted three times with ethyl acetate (EtOAc) and dried with MgSO<sub>4</sub>. The resulting crude mixture underwent analysis using GC-MS and <sup>1</sup>H-NMR, with conversions calculated based on GC-MS results.

### **3.3 Electrode cleaning process**

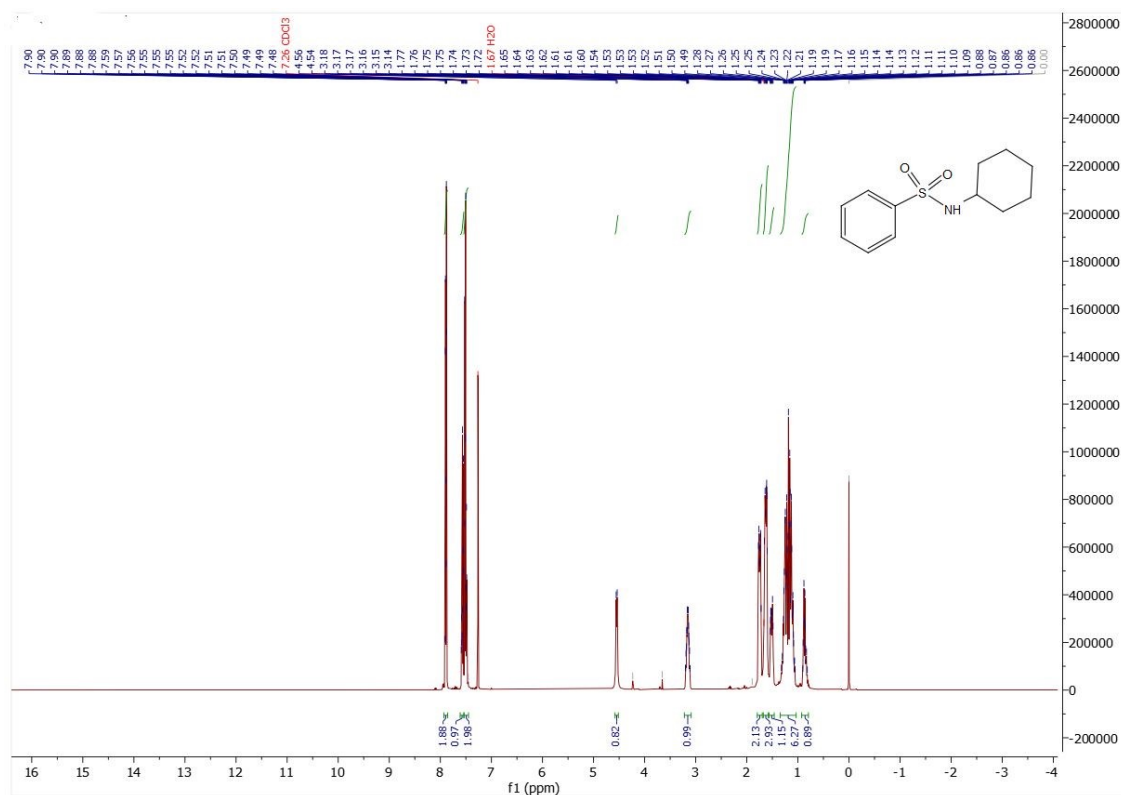
The stainless-steel electrode, graphite electrode, and Delrin cap underwent a thorough cleaning process. Initially, they were washed with acetone and scrubbed with a sponge twice. Subsequently, the electrodes were immersed in a beaker filled with deionized water and sonicated for 10 minutes, with this step repeated twice. Following this, the electrodes were placed in a beaker containing a 5% mucosol solution and sonicated for 15 minutes, repeating the process twice. Next, they were immersed in a beaker with acetone and sonicated for 10 minutes, the step repeated twice. The final cleaning step involved washing with acetonitrile, sonicated for 15 minutes twice. Afterward, the electrodes were wiped with cotton and left to air dry.

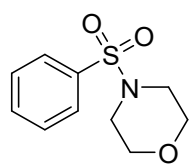
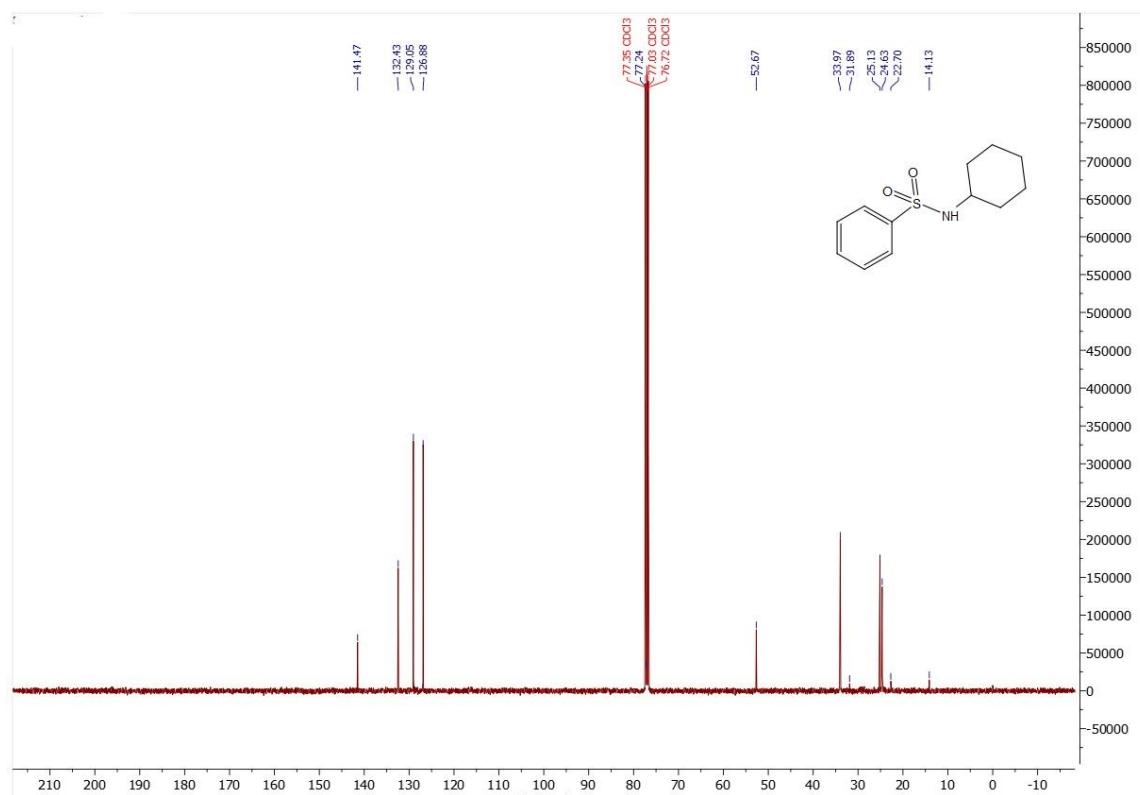
## 4. NMR characterization and spectra



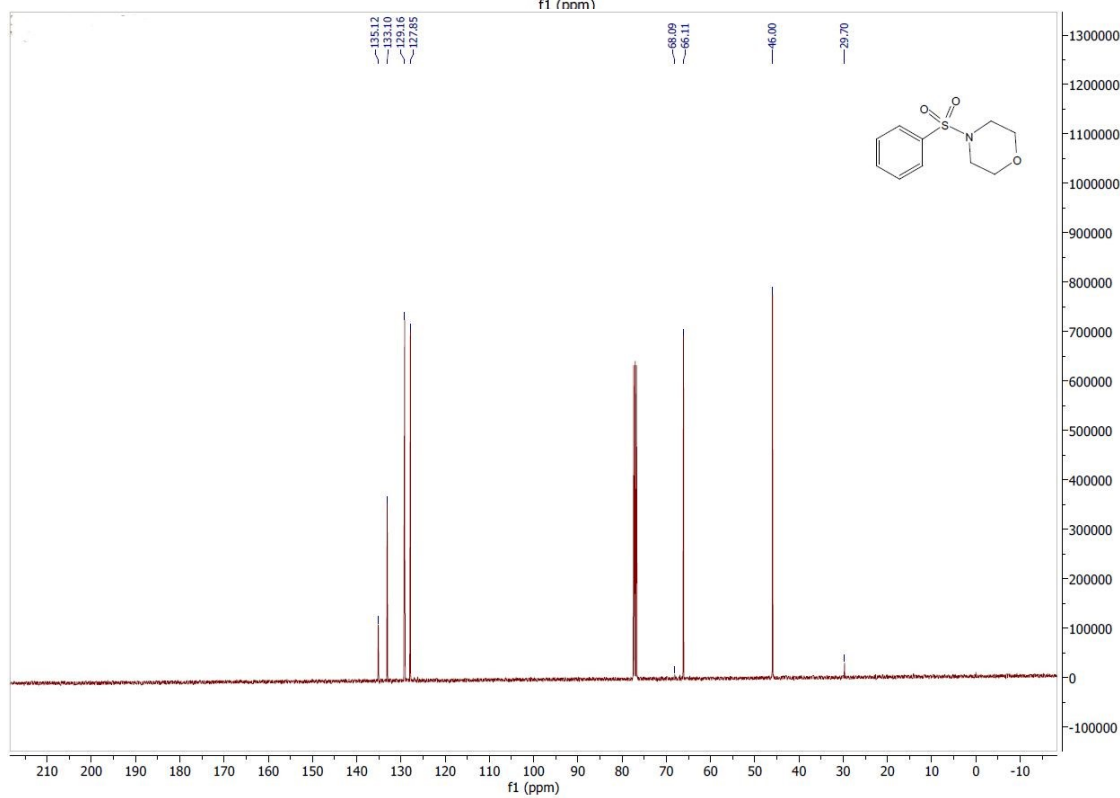
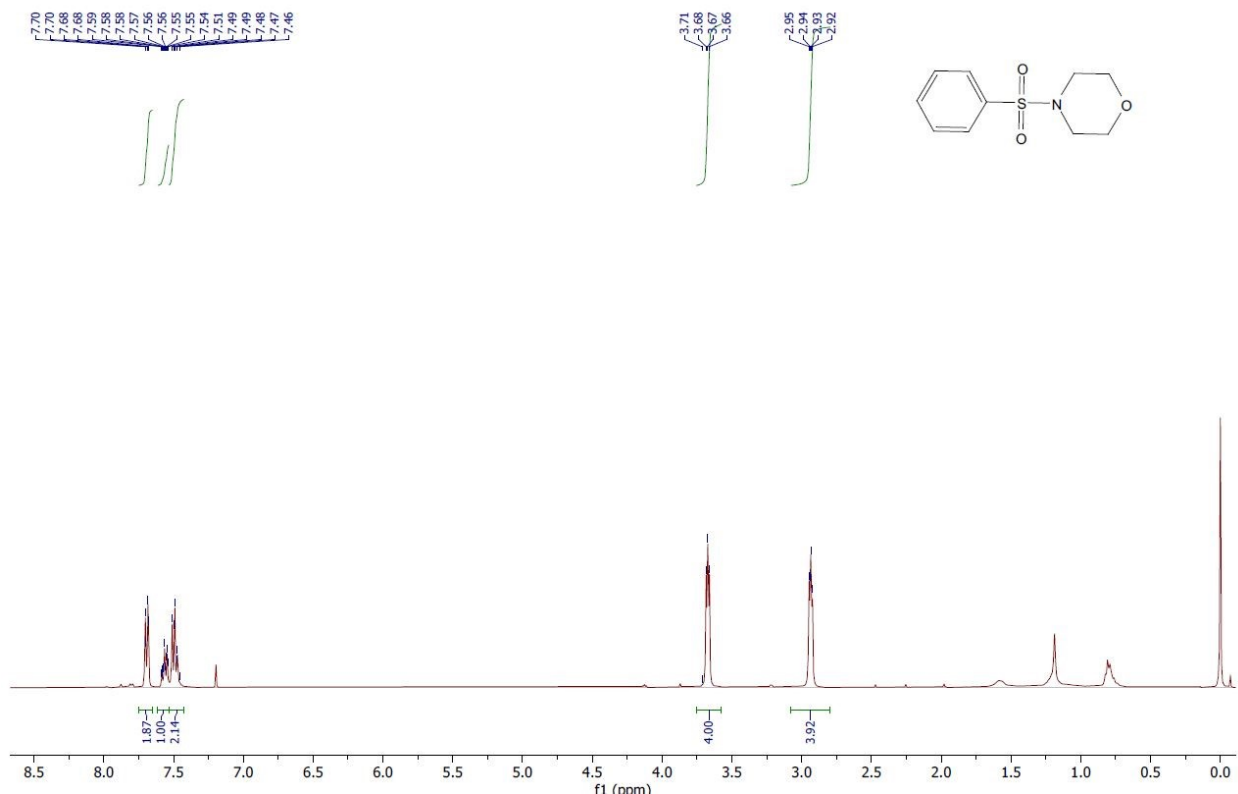
N-cyclohexylbenzenesulfonamide (**12**)-Isolated as off-white solid in 50% yield

(119 mg, 0.5 mmol)  $^1\text{H-NMR}$  (400 MHz, Chloroform- $d$ )  $\delta$  7.95 – 7.85 (m, 2H), 7.59 – 7.53 (m, 1H), 7.53 – 7.46 (m, 2H), 4.82 (d,  $J = 7.6$  Hz, 1H), 3.14 (ddq,  $J = 9.7, 6.6, 3.6$  Hz, 1H), 1.79 – 1.69 (m, 2H), 1.66 – 1.57 (m, 2H), 1.54 – 1.44 (m, 1H), 1.29 – 1.04 (m, 5H).  $^{13}\text{C}\{^1\text{H}\}$  NMR (100 MHz, Chloroform- $d$ )  $\delta$  141.6, 132.5, 129.1, 127.0, 52.8, 34.0, 25.2, 24.7 Mass spectra ( $\text{M}^+$ ) for  $\text{C}_{12}\text{H}_{17}\text{NO}_2\text{S}$ : 239.1.

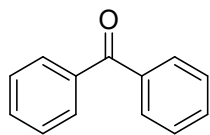




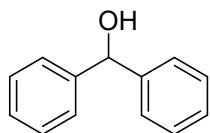
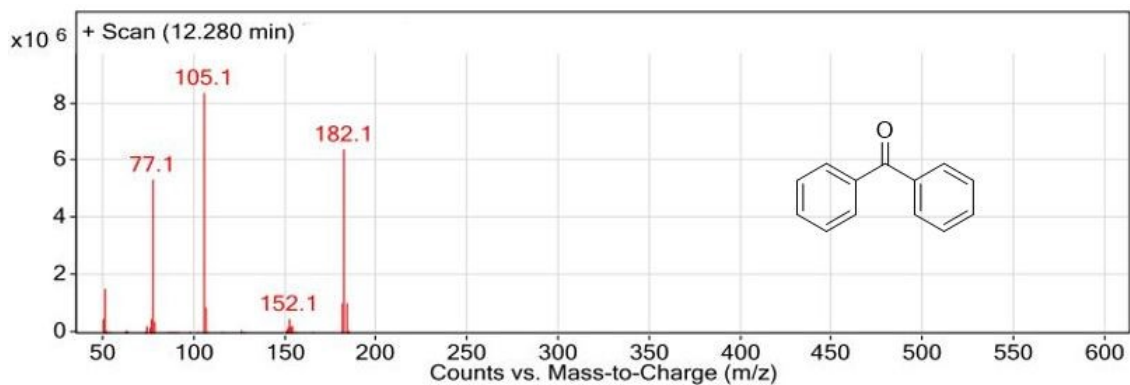
1-(phenylsulfonyl)morpholine (**14**)-Isolated to give a light brown solid (92 mg, 40%).  $^1\text{H-NMR}$  (399 MHz, Chloroform- $d$ )  $\delta$  7.79 – 7.72 (m, 2H), 7.66 – 7.59 (m, 1H), 7.59 – 7.51 (m, 2H), 3.76 – 3.70 (m, 4H), 3.03 – 2.96 (m, 4H) ppm.  $^{13}\text{C}\{^1\text{H}\}$  NMR (100 MHz, Chloroform- $d$ )  $\delta$  135.2, 133.2, 129.3, 127.9, 66.2, 46.1. Mass spectra ( $\text{M}^+$ ) for  $\text{C}_{10}\text{H}_{11}\text{NO}_3\text{S}$ : 227.



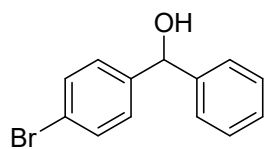
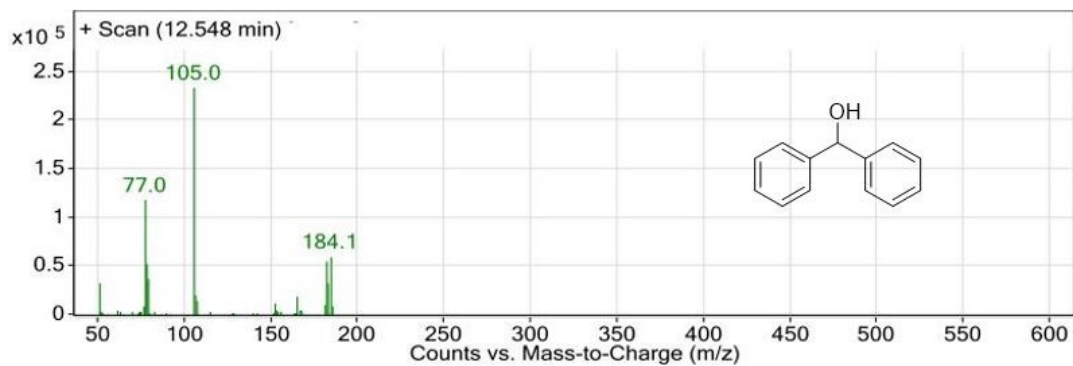
## 5.0 Mass Spectrometry data



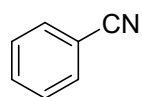
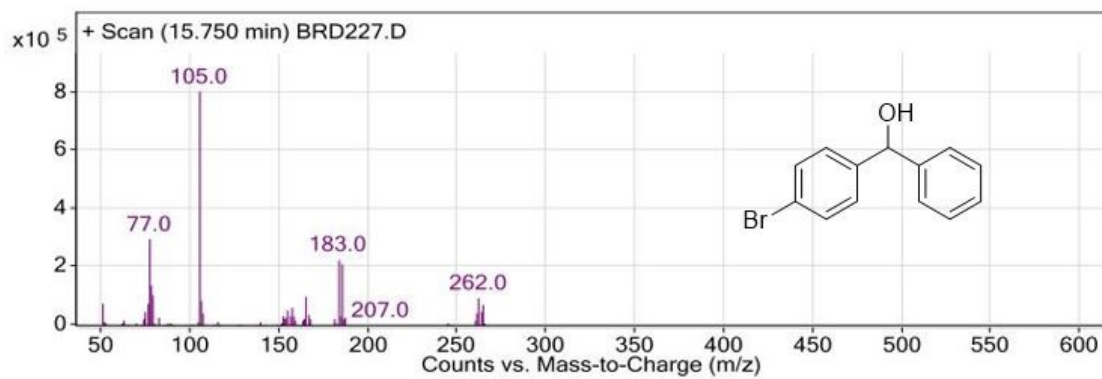
Benzophenone (**1**)-Mass spectra (M)<sup>+</sup> for C<sub>13</sub>H<sub>10</sub>O: 182.



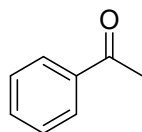
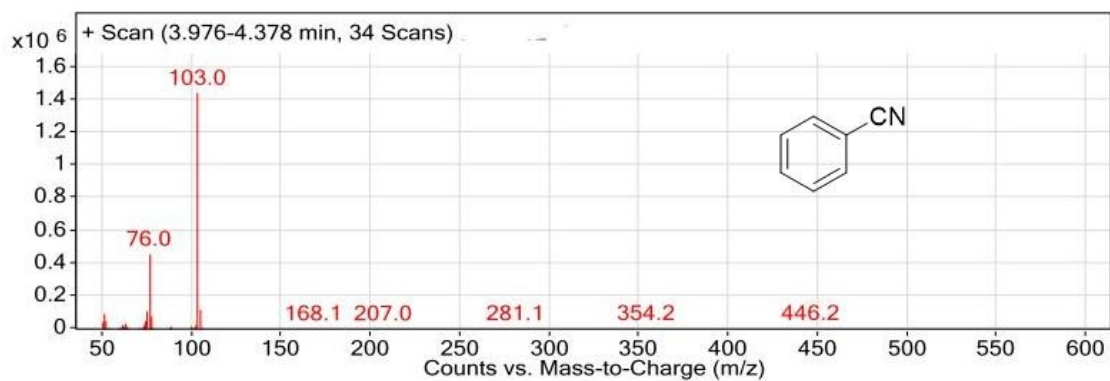
Diphenylmethanol (**2**)-Mass Spectra (M)<sup>+</sup> for C<sub>13</sub>H<sub>12</sub>O: 184.



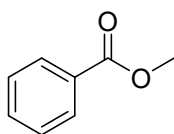
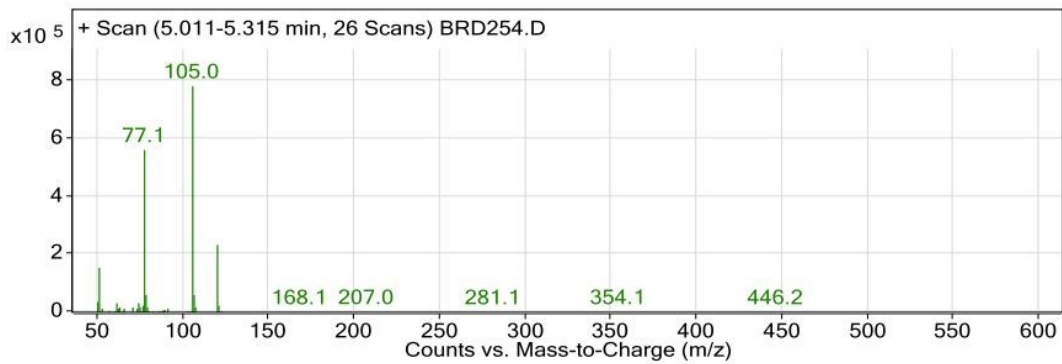
4-Bromobenzohydrol (**4**)-Mass spectra (M)<sup>+</sup> for C<sub>13</sub>H<sub>11</sub>BrO: 263.



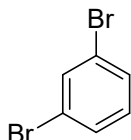
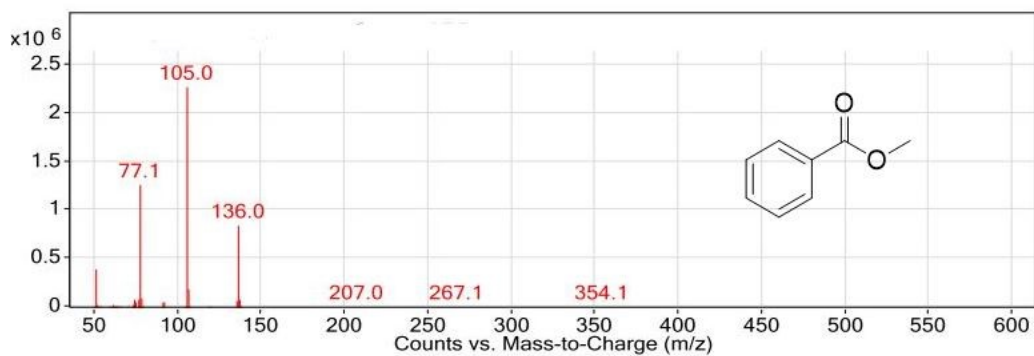
4-Bromobenzonitrile (**5**)-Mass spectra (M)<sup>+</sup> for C<sub>7</sub>H<sub>5</sub>N: 103.



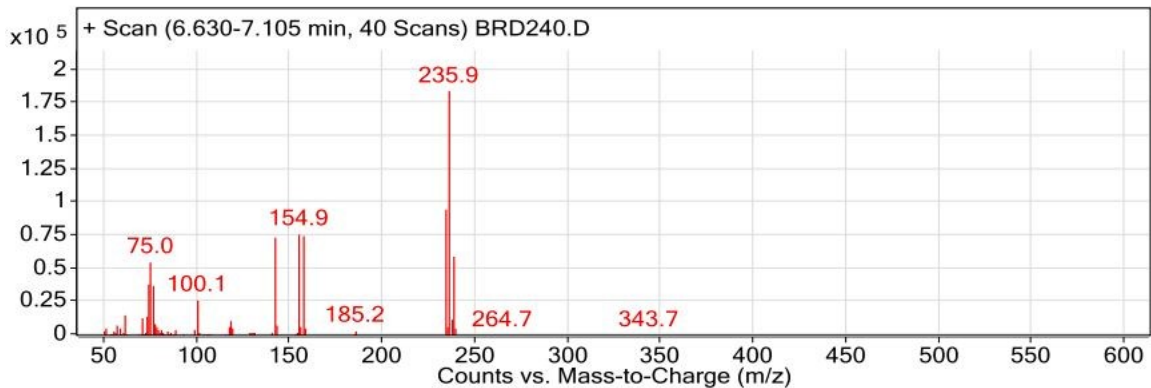
Acetophenone (**6**)-Mass spectra (M)<sup>+</sup> for C<sub>8</sub>H<sub>8</sub>O: 120.

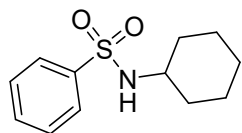


Methylbenzoate (**7**)-Mass spectra (M)<sup>+</sup> for C<sub>8</sub>H<sub>8</sub>O<sub>2</sub>:136.



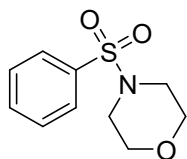
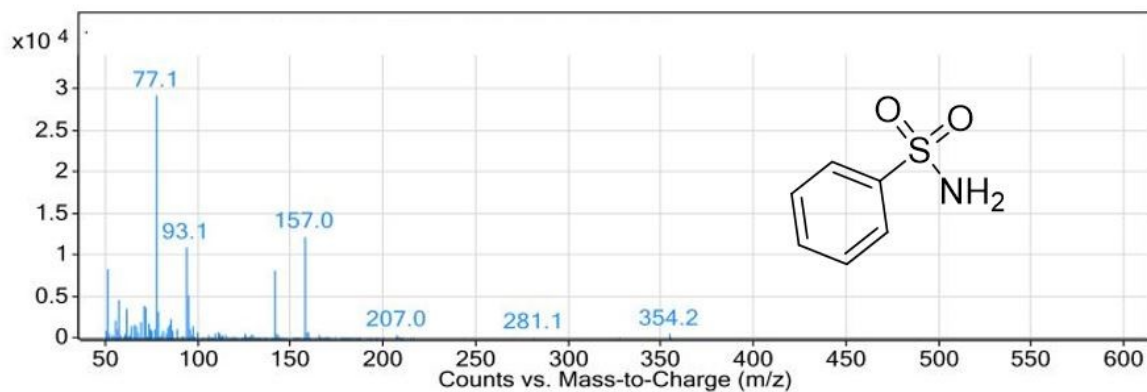
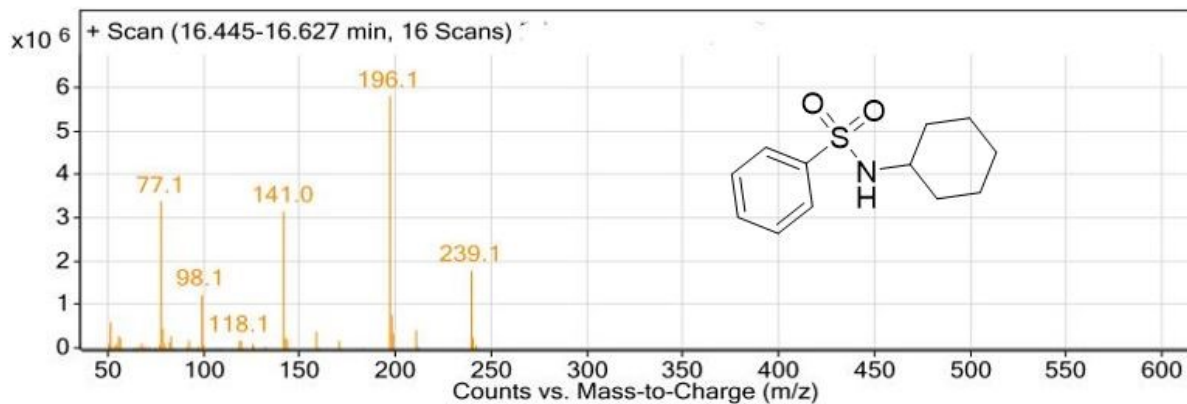
Dibromobenzene (**8**)-Mass spectra (M)<sup>+</sup> for C<sub>6</sub>H<sub>4</sub>Br<sub>2</sub>: 235.



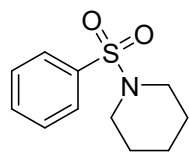
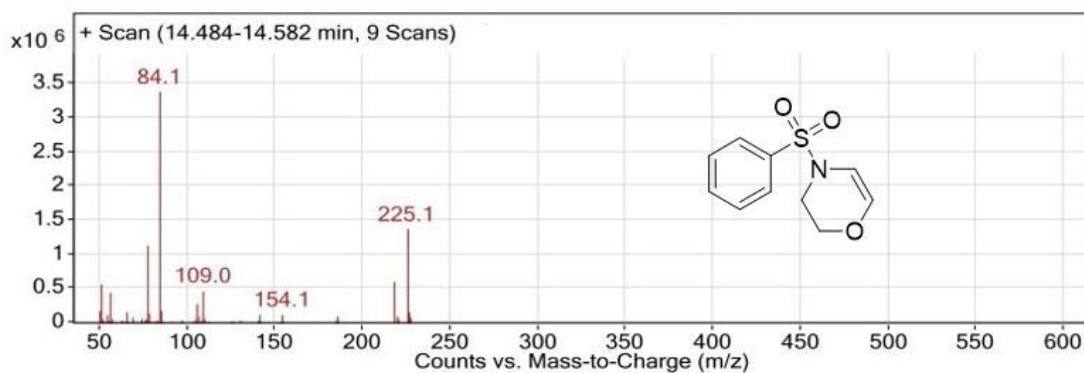
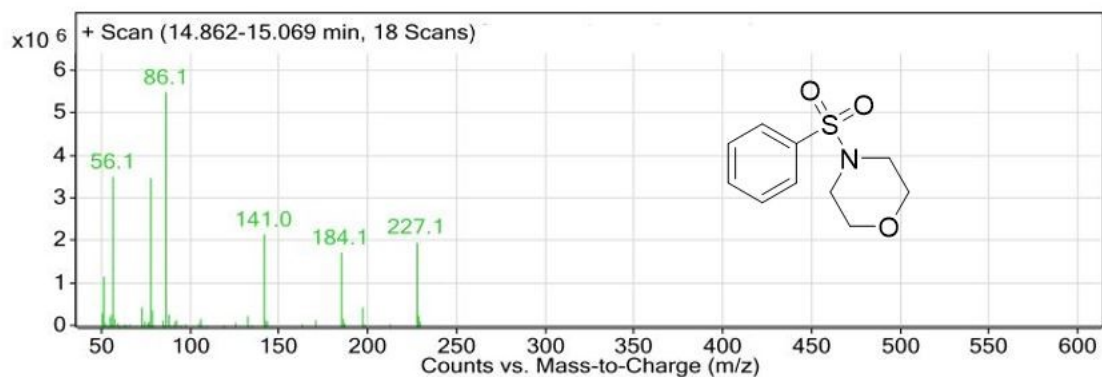


N-cyclohexylbenzenesulfonamide (**12**)- Mass spectra (M)<sup>+</sup> for C<sub>12</sub>H<sub>17</sub>NO<sub>2</sub>S:

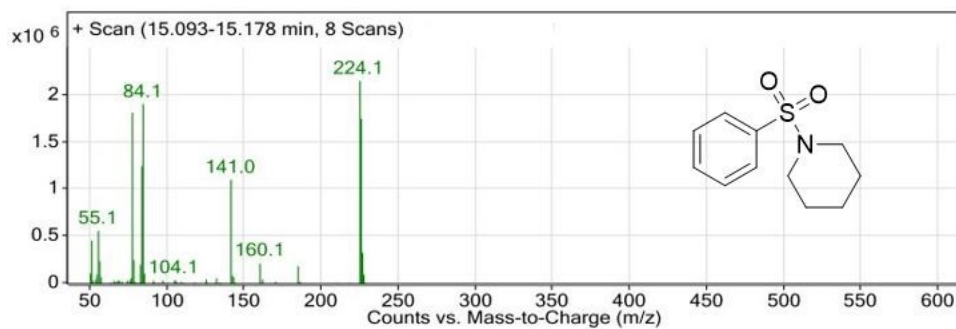
239.

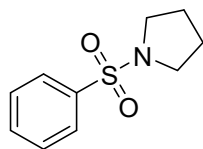
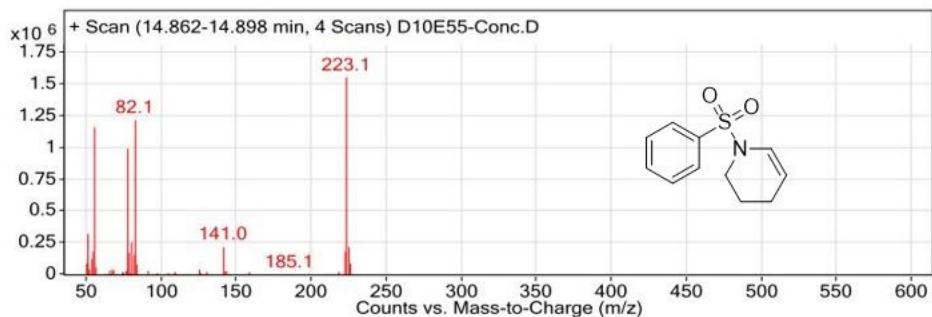


1-(phenylsulfonyl)morpholine (**14**) Mass spectra (M)<sup>+</sup> for C<sub>10</sub>H<sub>11</sub>4NO<sub>3</sub>S: 227.

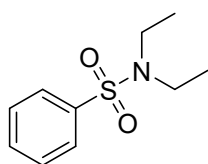
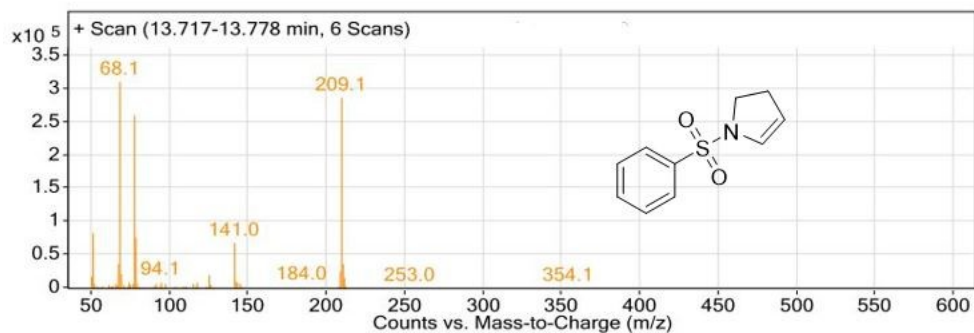
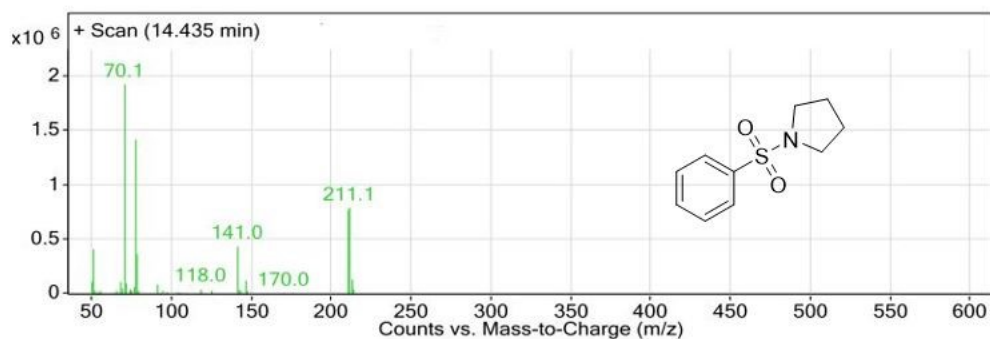


1-(phenylsulfonyl)piperidine (**15**) Mass spectra (M)<sup>+</sup> for C<sub>11</sub>H<sub>15</sub>NO<sub>2</sub>S: 225.

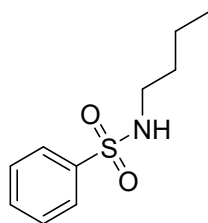
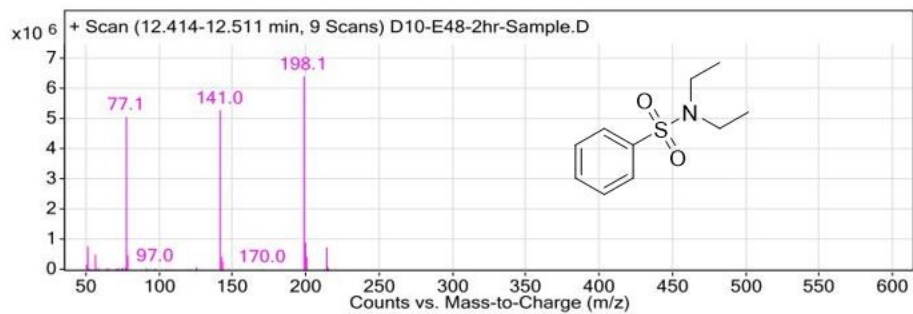




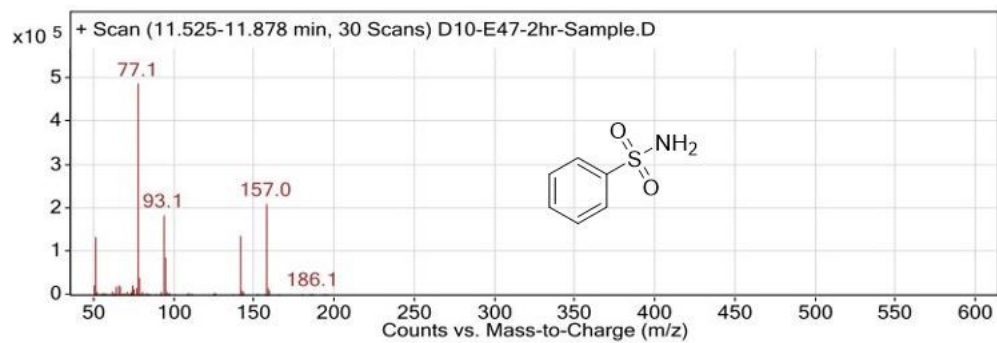
1-(phenylsulfonyl)pyrrolidine (**16**)-Mass spectra (M)<sup>+</sup> for C<sub>10</sub>H<sub>13</sub>NO<sub>2</sub>S: 211.

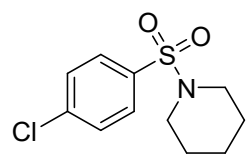
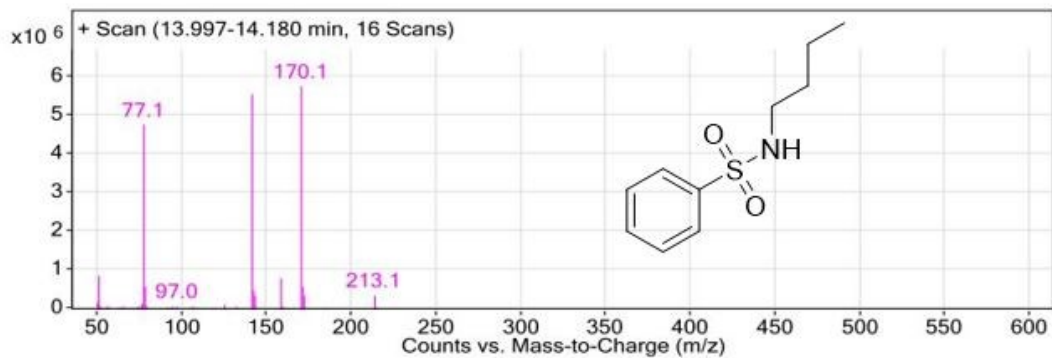
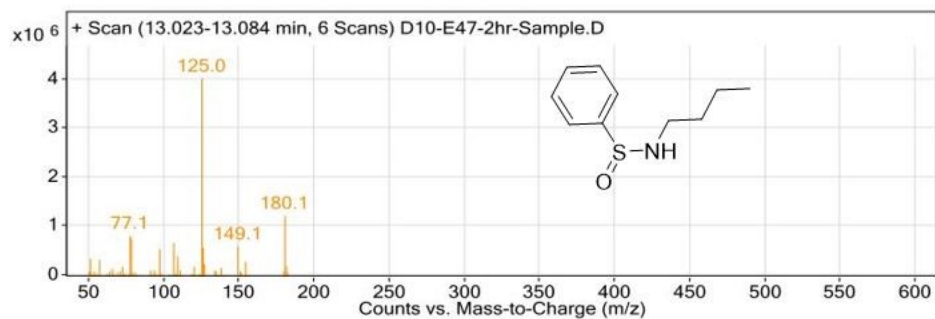


N,N-diethylbenzenesulfonamide (**17**)-Mass spectra (M)<sup>+</sup> for C<sub>10</sub>H<sub>15</sub>NO<sub>2</sub>S: 213.



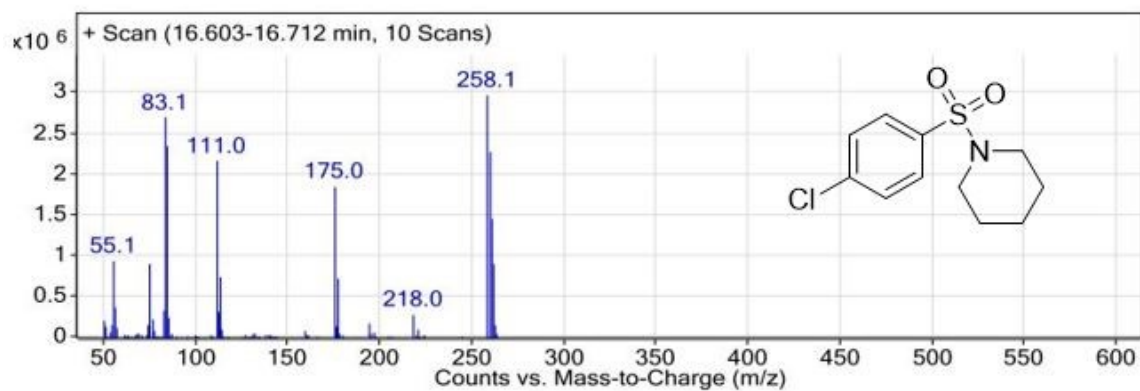
N-butylbenzenesulfonamide (**18**)-Mass spectra (M)<sup>+</sup> for C<sub>10</sub>H<sub>15</sub>NO<sub>2</sub>S: 213.08.

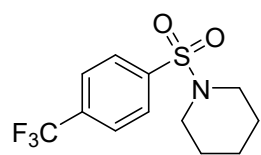
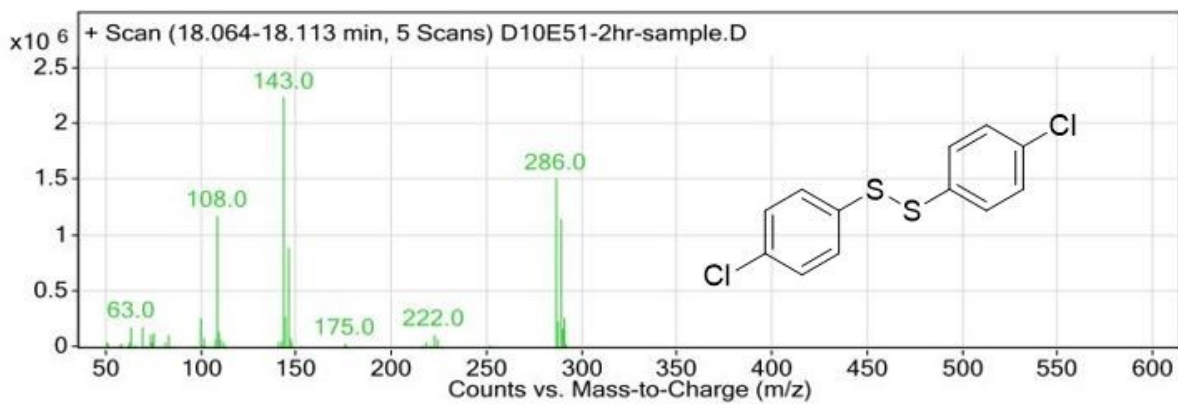




1-(4-chlorophenylsulfonyl)piperidine (19)-Mass spectra (M)<sup>+</sup> for

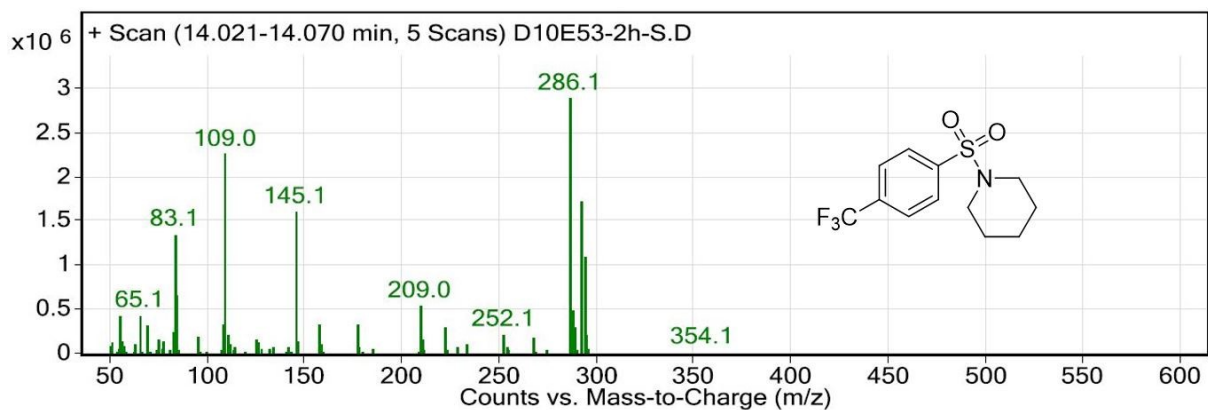
C<sub>11</sub>H<sub>14</sub>ClNO<sub>2</sub>S: 259.

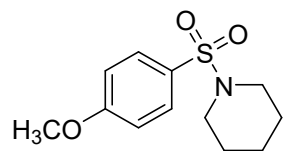
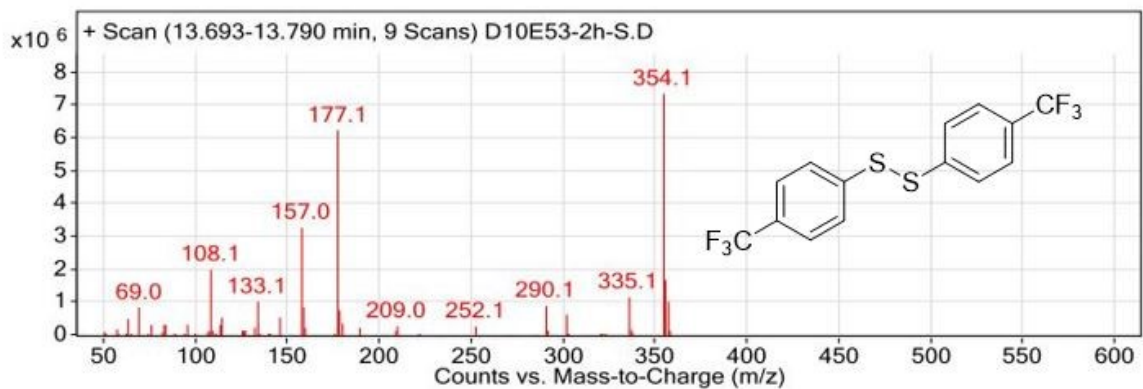




1-(4-(trifluorophenyl)sulfonyl)piperidine (**20**) -Mass spectra (M)<sup>+</sup> for

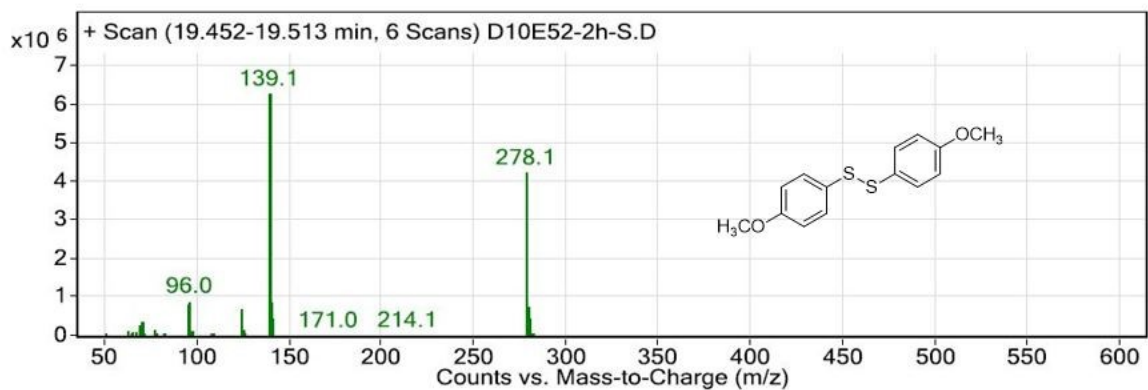
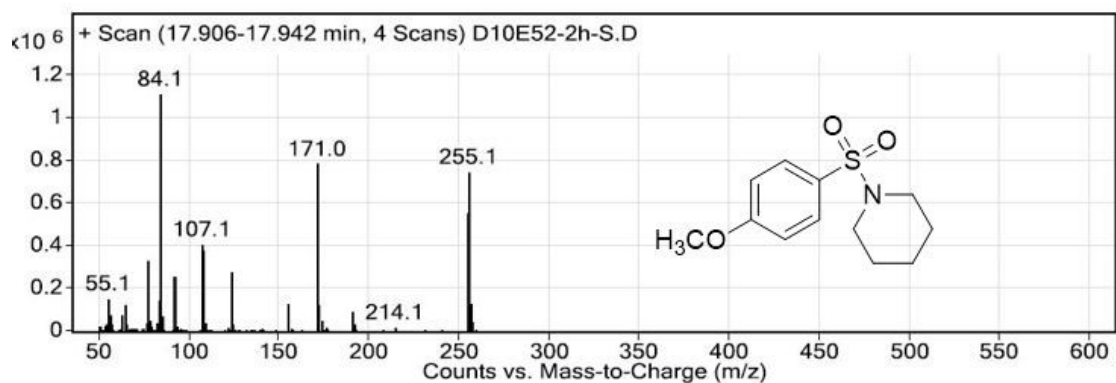
$C_{12}H_{14}F_3NO_2S$ : 293.

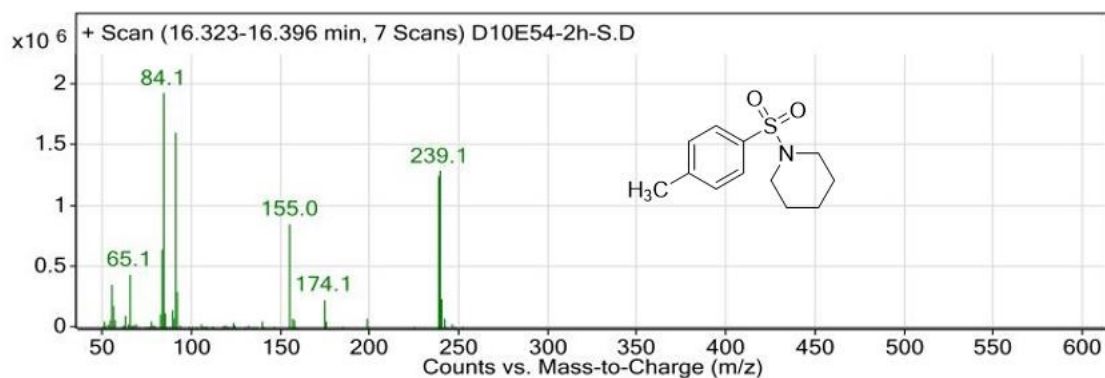
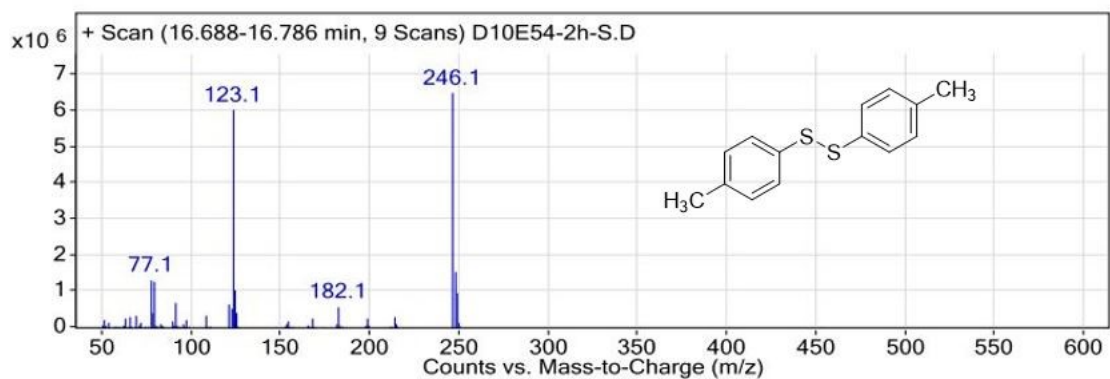
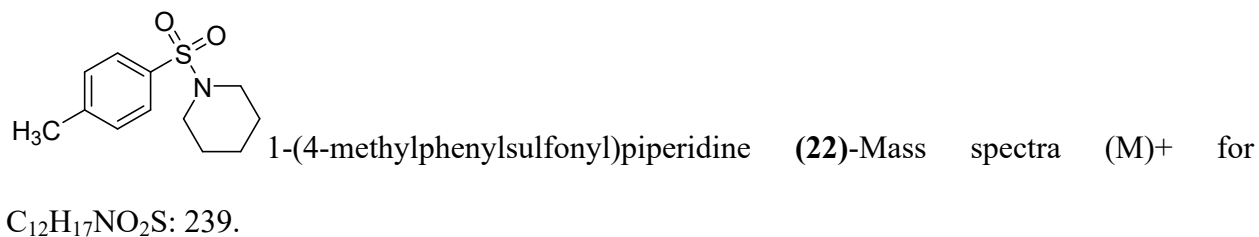




1-(4-methoxyphenylsulfonyl)piperidine (**21**)-Mass spectra (M)<sup>+</sup> for

C<sub>12</sub>H<sub>17</sub>NO<sub>3</sub>S: 255.





## 6. Green metrics calculation

### 6.1 Atom Economy (AE)

$$AE(\%) = \frac{\text{Molecular weight of product}}{\text{Total molecular weight of reactants}} \times 100$$

### 6.2 Reaction Mass Efficiency (RME)

$$RME(\%) = \frac{\text{Mass of isolated product}}{\text{Total mass of reactants}} \times 100$$

### 6.3 Process Mass Intensity (PMI)

$$PMI = \frac{\text{Total mass in a process}}{\text{Mass of product}}$$

### 6.4 Calculations for Oxidative coupling for sulfonamide synthesis procedure

Table S6. Values used to calculate the quantitative green metrics for electrochemical oxidative coupling of thiophenol and cyclohexylamine. These estimated values are based on reported literature and from the current method. The calculation was conducted with the help of the Process Mass Intensity Calculator tool provided by the green chemistry institute pharmaceutical roundtable chemistry innovation tools.<sup>4</sup>

	New method	Previous method (Batch reactor) <sup>3</sup>	Previous method (microflow cell) <sup>3</sup>
Scale (mmol)	1	3	10
Thiophenol (g)	0.11017	0.33051	1.1
N-Cyclohexylamine (g)	0.148755	0.446265	1.5
Bu <sub>4</sub> NPF <sub>6</sub> (g)	0.04	-	-
Me <sub>4</sub> NBF <sub>4</sub> (g)	-	0.04	0.16
Acetonitrile (g)	1.2	18	58
0.3 M HCl (g)	0.5	7.5	25
N-Cyclohexylaminesulfonamide(g)	0.12	0.4	1.9
% Yield	50	55	80
% AE	100	100	100
% RME	46.2	50.8	34.1
% OE	46.2	50.8	34.1
PMI Substrate reagents (g/g <sup>-1</sup> )	2.5	2.1	3
PMI Solvent (g/g <sup>-1</sup> )	9.8	46.2	31
PMI Aqueous (g/g <sup>-1</sup> )	4.2	19.2	13
PMI (g/g <sup>-1</sup> )	16.4	67.5	47

## 7. Reference

1. S. Maljuric, W. Jud, C. O. Kappe, D. Cantillo, J Flow Chem 2020, 10 (1), 181–190.
2. H. Roth, N. Romero, D. Nicewicz, Synlett 2015, 27 (05), 714–723.
3. G. Laudadio, E. Barmpoutsis, C. Schotten, L. Struik, S. Govaerts, D. L. Browne, T. Noël, J Am Chem Soc 2019, 141 (14), 5664–5668.
4. <https://www.acsgcipr.org/tools-for-innovation-in-chemistry/> (accessed 20 May 2024)